

Rapidly Rotating Bose-Einstein Condensates

Gordon Baym

*Department of Physics, University of Illinois at Urbana-Champaign
1110 West Green Street, Urbana, Illinois 61801*

How does a rapidly rotating condensed Bose gas carry extreme amounts of angular momentum? The energetically favored state of a not-too-rapidly rotating Bose condensed gas is, as observed, a triangular lattice of singly quantized vortices. This paper describes the fates of the vortex lattice in both harmonic and anharmonic traps when condensates are rotated extremely rapidly.

PACS numbers: 03.75.Lm, 67.40.Db, 67.40.Vs, 05.30.Jp

1. INTRODUCTION

Superfluids respond to rapid rotation by forming triangular arrays of singly quantized vortex lines. Compared with superfluid ^4He ,¹ the properties of vortices in Bose-Einstein condensed atomic gases have proven to be considerably more accessible. Following the creation of single vortex lines in atomic condensates by phase imprinting,² large arrays have been created via mechanical rotation, by stirring the condensate with a laser beam,^{3,4} and by particle evaporation.⁵ Upwards of 300 vortex lines have been created in rapidly rotating condensates, and properties such as the modes of the lattice^{6,7} and vortex core structure^{7,8} have been studied in detail.

The superfluid velocity, \vec{v} , obeys the quantization condition, $\oint \vec{v} \cdot d\vec{\ell} = (h/m)N_v(\mathcal{C})$, where the line integral is along a closed contour surrounding $N_v(\mathcal{C})$ singly quantized vortices, h is Planck's constant, and m the particle mass. In the neighborhood of a single line, the velocity is in the azimuthal direction and has magnitude $\hbar/m\rho$, where ρ is the distance from the line. A system containing many vortex lines appears to rotate uniformly with an average angular velocity Ω , which is simply related to the (two-dimensional) density of vortex lines, n_v , by the quantization condition: $\Omega = \pi\hbar n_v/m$. As the system rotates more and more rapidly, the lines become closer and closer.

G. Baym

The question I would like to discuss here is what eventually happens to the vortex array. In other words, how does a rapidly rotating Bose condensate carry large quantities of angular momentum per particle?

One may be tempted to argue by analogy with a Type II superconductor which in the presence of a magnetic field above a critical value, H_{c1} , contains an array of vortex lines with quantized flux. As the field is increased the line density grows until the cores begin to overlap, at a critical field, H_{c2} , at which point the system turns normal. However, a low temperature rotating bosonic system *does not* have a normal phase to which it can return.⁹ Unlike in a weakly interacting superconductor, where condensation occurs as a small dynamical decoration on top of a normal state, Bose condensation occurs kinematically. A Bose system must respond differently than a Type II superconductor. In He II, the question has never been of experimental interest, since the intervortex spacings are typically macroscopic, while the core sizes are of order Ångströms, and thus the critical rotation rate, Ω_{c2} , at which the vortex cores would approach each other is unobservably large, $\sim 10^{12}$ rad/sec.¹⁰ In a weakly interacting atomic condensate, the radius of a single vortex core is of order $\xi_0 = 1/\sqrt{8\pi na}$, where a is the s-wave scattering length, and n is the particle density. Typically, $\xi_0 \sim 0.2 \mu\text{m}$, so that cores would begin to touch at $\Omega_{c1} \sim 8\pi^2 na\hbar/m \sim 10^3 - 10^5$ rad/sec, an experimentally accessible rate.

The ground state of the system rotating at angular frequency Ω about the z axis is determined by minimizing the energy in the rotating frame, $E' = E - \Omega L_z$, where L_z is the component of the angular momentum of the system along the rotation axis:

$$E' = \int d^3r \left[\frac{\hbar^2}{2m} |(-i\nabla - m\vec{\Omega} \times \vec{r})\psi|^2 + \left(V(\vec{r}) - \frac{1}{2}m\Omega^2 r_\perp^2 \right) |\psi|^2 + \frac{1}{2}g|\psi|^4 \right] \quad (1)$$

where ψ is the condensate wave function, $\vec{r}_\perp = (x, y)$, $V(\vec{r})$ is the trapping potential, and $g = 4\pi\hbar^2 a/m$ determines the strength of the interparticle interaction.

The fate of a rapidly rotating Bose system depends on how the system is confined. In typical condensate experiments the system, rotating about the z axis, is confined in a harmonic trap of the form,

$$V(r_\perp, z) = \frac{1}{2}m(\omega_\perp^2 r_\perp^2 + \omega_z z^2). \quad (2)$$

In this case the centrifugal potential, $-\frac{1}{2}m\Omega^2 r_\perp^2$, tends to cancel the transverse trapping potential, and the system cannot rotate faster than ω_\perp without becoming untrapped. As $\Omega \rightarrow \omega_\perp$, the system flattens out, becomes

Rapidly Rotating Bose-Einstein Condensates

almost two dimensional, and eventually enters quantum Hall-like states. On the other hand, in the presence of an anharmonic transverse trapping potential that grows faster than quadratic, e.g.,

$$V_{\perp}(r_{\perp}) = \frac{1}{2}m\omega_{\perp}^2 r_{\perp}^2 (1 + \lambda r_{\perp}^2), \quad (3)$$

the system can rotate faster than ω_{\perp} , since it is contained by the anharmonic part of the potential.

2. THE VORTEX CORES SHRINK WITH INCREASING Ω

In fact there is never a phase transition associated with the vortex cores overlapping in a rotating Bose condensate. Rather, as the intervortex spacing becomes comparable to the mean field coherence length, ξ_0 , the vortex cores begin to shrink, and eventually the core radius scales down with the intervortex spacing.

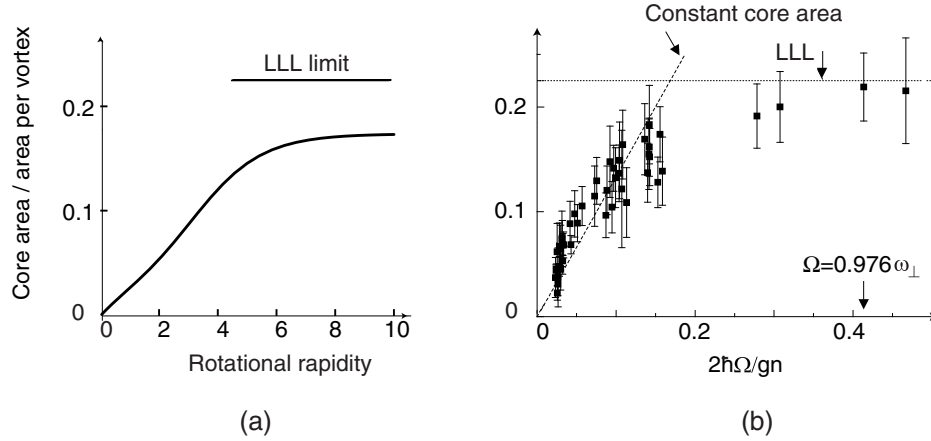


Fig. 1. (a) Mean vortex core area as a fraction of the area per vortex vs. the rotational rapidity (see text). (b) Measured vortex core area as a fraction of the area per vortex vs. $2\Omega/gn$. Adapted from Ref. 7.

In Ref. 11, and more fully in Ref. 12, we approached the problem by treating the core radius, ξ , as a variational parameter. By integrating out the short range structure on scales of the vortex separation, one derives an effective Hamiltonian,

$$E' = \int d^3r n(\vec{r}) \left[-\frac{\Omega^2}{2}mr^2 + V(\vec{r}) + a\hbar\Omega + \frac{1}{2}bgn(\vec{r}) \right], \quad (4)$$

G. Baym

where $n(\vec{r})$ is the smoothed density; the parameter $a(\xi)$ takes into account the local vortex kinetic energy, including the curvature of the order parameter, and $b(\xi)$ describes the renormalization the coupling constant, g , due to density fluctuations about the smoothed density within each vortex cell. The core size is determined by minimizing Eq. (4) with respect to ξ . Figure 1a shows the resultant mean square area of the vortex core, in a harmonic trap, measured in units of the area per vortex line, for the qualitatively accurate model in which the condensate wave function has the form $\psi(\rho) \sim \rho$, for $\rho < \xi$, and constant for $\xi < \rho < \ell$, where ℓ is the radius of the (cylindrical) Wigner-Seitz cell around a given vortex: $\ell^2 = 1/m\Omega$. In this model, the mean square core area divided by the area per vortex, \mathcal{A} , is $\xi^2/3\ell^2$. The horizontal axis in Fig. 1 is the rotational rapidity,¹² y , defined by $\Omega/\omega_\perp = \tanh y$, a convenient variable for spreading out the region where $\Omega \lesssim \omega_\perp$. The linear rise at small Ω occurs because the core size remains constant, while ℓ^2 decreases linearly with $1/\Omega$. The flattening of \mathcal{A} with increasing Ω is a consequence of the vortex radius scaling with the inter-vortex spacing. The upper line shows the exact limit as $\Omega \rightarrow \omega_\perp$. Recent JILA measurements^{7,8} of \mathcal{A} (as a function of $2\hbar\Omega/gn$), Fig. 1b, nicely show the expected initial linear rise, followed by the predicted scaling of the core radius with intervortex spacing.

3. LOWEST LANDAU LEVEL REGIME

As the rotation rate in a harmonic trap approaches ω_\perp , the centrifugal potential basically cancels the transverse trapping potential; the cloud flattens out, and becomes an effectively two dimensional system. Because the density n of the system drops, the interaction terms $\sim gn$, become small compared with $\hbar\Omega$. Then, as one sees from Eq. (1) with (2), the dynamics is that of a particle feeling the Coriolis force alone, a system formally analogous to a particle in a magnetic field. Ho¹³ predicted that in this limit particles should condense into the lowest Landau level (LLL) in the Coriolis force, similar to charged particles in the quantum Hall regime. When $2gn \ll \Omega$, the states in the next higher Landau level are separated by a gap $\simeq 2\omega_\perp$. This insight has led to extensive experimental studies in which rotation rates in excess of $0.99 \omega_\perp$ have been achieved.^{5,7}

The single particle wave functions in the lowest Landau level have the form, $\phi_\mu(\vec{r}_\perp) \sim \zeta^\mu e^{-r_\perp^2/2d_\perp^2}$, where $\zeta = x + iy$, $\mu = 0, 1, 2, \dots$, and the transverse oscillator length, d_\perp , is given by $\sqrt{\hbar/m\omega_\perp}$. The LLL condensate

Rapidly Rotating Bose-Einstein Condensates

wave function is a linear superposition of such states:

$$\phi_{\text{LLL}}(\vec{r}_\perp) \sim \sum_\mu c_\mu \zeta^\mu e^{-r^2/2d_\perp^2} \sim \prod_{i=1}^N (\zeta - \zeta_i) e^{-r^2/2d_\perp^2}, \quad (5)$$

where the polynomial $\sum_\mu c_\mu \zeta^\mu$ is written as a product over its zeroes, ζ_i , which are simply the positions of the vortices in the condensate. The state (5) in the regime $gn \ll \hbar\Omega$ is a direct continuation of the state in the slowly rotating regime, $\hbar\Omega \ll gn$.

4. DENSITY PROFILE AND LATTICE DISTORTION

As long as the total number of vortices is much larger than unity, the energy of the cloud in the LLL limit is given by¹⁴

$$E' = \Omega N + \int d^3r \{ (\omega_\perp - \Omega) \frac{r_\perp^2}{d_\perp^2} n(\vec{r}) + \frac{bg}{2} n(\vec{r})^2 \}, \quad (6)$$

plus terms involving the trapping potential in the z direction. Here $n(\vec{r})$ is the smoothed density profile, $= \langle |\phi_{\text{LLL}}|^2 \rangle$; the brackets denote the long wavelength smoothing. The energy (6) is minimized when the cloud assumes a density profile of the Thomas-Fermi form,¹⁵ $n(r_\perp) \sim (1 - r_\perp^2/R^2)$ – an inverted parabola – where R is the transverse radius of the cloud. For $Na/d_z \gg 1$, where d_z is the axial oscillator length, the structure in the radial direction will be Thomas-Fermi at large Ω , even if it is Gaussian at small Ω .¹² In experiment,^{7,8} the density profile indeed remains an inverted parabola as $\Omega \rightarrow \omega_\perp$.

Since the energy (6) depends only on the smoothed density, the vortices must adjust their locations in order that the smoothed density be an inverted parabola. From the arguments in Ref. 13, we find the relation between the smoothed density and the mean vortex density, $n_v(r_\perp)$,

$$\frac{1}{4} \nabla^2 \ln n(r_\perp) = -\frac{1}{d_\perp^2} + \pi n(r_\perp). \quad (7)$$

For a Gaussian density profile, the vortex density is constant. However, for a Thomas-Fermi profile,

$$n_v(r_\perp) = \frac{1}{\pi d_\perp^2} - \frac{1}{\pi R^2} \frac{1}{(1 - r_\perp^2/R^2)^2}. \quad (8)$$

Since the second term is of order $1/N_v$ compared with the first, the density of the vortex lattice is basically uniform (and the vortex array forms an

G. Baym

almost perfect triangular lattice). Turning the argument around, very small distortions of the vortex lattice from triangular can result in large changes in the density distribution.¹⁶ Recent measurements of the (percent scale) distortions of the vortex lattice at relatively low rotation rates,⁸ are in good agreement with theory.

5. LATTICE MODES

The collective modes of the vortex lattice in a rotating superfluid have been of considerable interest since the 1960's, when Tkachenko¹⁸ showed that the lattice supports an elliptically polarized mode, a mode observed in helium in 1982.¹⁹ To describe the Tkachenko modes, Ref. 20 reformulated the hydrodynamics of rotating superfluids to take into account the elasticity of the vortex lattice (including normal fluid, dissipation, and line bending – Kelvin – oscillations of the vortex lines in three dimensions); effects of the oscillations of the vortex lines at finite temperature on the long range phase correlations of the superfluid were discussed in Ref. 21. In superfluid helium, where Ω is always much smaller than characteristic phonon frequencies, $sk \sim s/R$, where s is the sound velocity and R the transverse size, the modes frequencies are linear in the wave vector, $\omega_T = (2C_2/mn)^{1/2}k$, where C_2 , the shear modulus, equals $\hbar n\Omega/8$. However, in Bose condensates it is possible to go to the rapidly rotating regime^{6,7,8} where $\Omega > sk$. For general Ω , the in-plane Tkachenko mode frequencies are given by,^{22,23}

$$\omega_T^2 = \frac{2C_2}{nm} \frac{s^2 k^4}{\{4\Omega^2 + (s^2 + 4(C_1 + C_2)/nm)k^2\}}, \quad (9)$$

where C_1 is the compressional modulus of the vortex lattice. Note that at low k , the mode frequency becomes $\sim k^2$. In addition the system supports a gapped sound mode of frequency,

$$\omega_I^2 = 4\Omega^2 + \left(s^2 + \frac{4}{nm}(C_1 + C_2) \right) k^2. \quad (10)$$

Figure 2a shows the frequencies as a function of k , while Fig. 2b shows the lowest mode frequency (of wave vector¹⁷ $5.45/R$) evaluated for a trapped rotating ⁸⁷Rb gas of $N = 2.5 \times 10^6$ particles.²⁴ In experiment,^{6,7} the particle number varies from run to run; here we have multiplied the experimental frequencies by a factor $(N/2.5 \times 10^6)^{-1/5}$ to compare with theory, calculated for $N = 2.5 \times 10^6$. As one approaches the LLL regime, the shear modulus decreases to^{23,25} $C_2 \simeq (81/80\pi^4)ms^2n$; the Tkachenko modes are then softer by a factor $(9/\pi^2)(ms^2/10\Omega)^{1/2}$; see solid curve in Fig. 2a. This softening

Rapidly Rotating Bose-Einstein Condensates

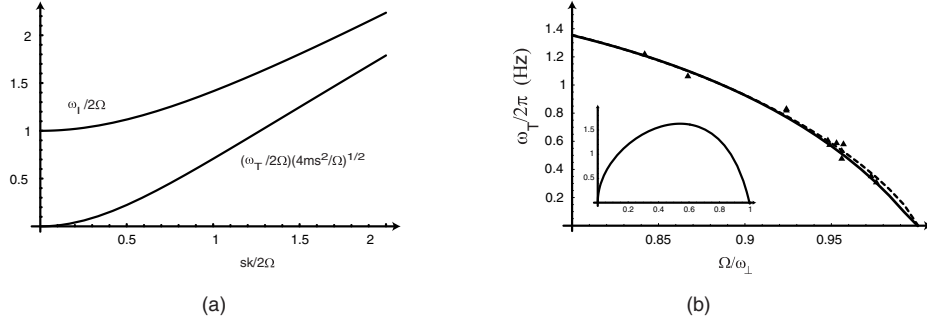


Fig. 2. a) Gapped sound and Tkachenko mode frequencies vs. wavevector, for $\Omega \ll ms^2$. (b) Frequency of the lowest Tkachenko mode, with the mean sound velocity, a decreasing shear modulus, C_2 (solid curve) and a constant C_2 (dashed curve). The data (triangles) are from Ref. 6. The inset shows ω_T over the entire range of Ω , at constant C_2 .

of the modes has recently been measured,^{7,8} and is in good agreement with theory.

The softness of the Tkachenko modes in the rapidly rotating regime leads to infrared singular behavior in the vortex transverse displacement-displacement correlations at finite temperature, and in the order parameter phase correlations even at zero temperature.^{23,25,26} The zero point oscillations of the vortices cause quantum melting of the lattice when $N_v \sim 10 - 20N$, where N_v is the total number of vortices present.^{23,25} In a finite system the single particle density matrix, $\langle \psi(r)\psi^\dagger(r') \rangle$, falls algebraically as $|\vec{r} - \vec{r}'|^{-\eta}$, where²³ $\eta \simeq (ms^2n/8C_2)^{1/2}N_v/N$. Dephasing of the condensate becomes significant only as $N_v \rightarrow N$, and not necessarily before the vortex lattice melts.

However, in three dimensions, the Tkachenko mode frequency at long wavelengths becomes linear in the wavevector for any propagation direction out of the transverse plane.²⁶ At zero temperature the vortex displacement correlations are convergent at large separation, but at finite temperatures, they grow with separation. The growth of the vortex displacements should lead to observable melting of vortex lattices at higher temperatures and somewhat lower particle number and faster rotation than in current experiments. At zero temperature a system of large extent in the axial direction maintains long range order-parameter correlations for large separation, but at finite temperatures the correlations decay with separation.²⁶

G. Baym

6. BEYOND THE LLL REGIME

At sufficiently high rotation, the vortex lattice should melt and become a vortex liquid. The regime just beyond melting has yet to be described in detail. At still higher rotation speeds, as seen in numerical simulations with a limited number of particles, the system begins to enter a sequence of highly correlated incompressible fractional quantum Hall-like states.^{27,28,29,30} For example, at angular momentum $L_z = 2N(N-1)$, where N_v (measured in terms of the total circulation, $N_v = (m/h) \oint \vec{v} \cdot d\vec{\ell}$) equals $2N$, the exact ground state is an N -particle fully symmetric Laughlin wave function (in two dimensions),

$$\Psi(r_1, r_2, \dots, r_N) \sim \prod_{i \neq j} (\zeta_i - \zeta_j)^2 e^{-\sum_k r_k^2 / 2d_\perp^2}, \quad (11)$$

where $\zeta_j = x_j + iy_j$. Since the wave function vanishes whenever two particles overlap, the interaction energy, $\frac{1}{2}g\sum_{i \neq j} \delta(\vec{r}_i - \vec{r}_j)$, vanishes in this state. Theoretically elucidating the states in general when the angular momentum per particle is of order the total particle number, as well as studying this regime experimentally, remain important challenges.

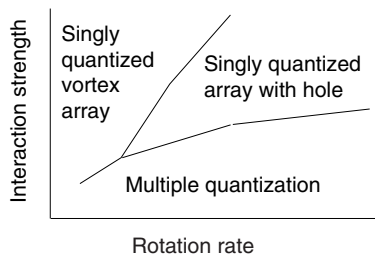


Fig. 3. Schematic phase diagram of the ground state of a rapidly rotating Bose condensed gas at zero temperature in the Ω - Na/Z plane, where Z is the height in the z direction, showing the regions of multiply quantized vortices, of singly quantized vortices forming an array which at large number becomes a triangular lattice, and of an array of singly quantized vortices with a hole in the center.

7. ANHARMONIC TRAPS

The physics of a condensate confined in an anharmonic trap, e.g., (3), is quite different from that in a harmonic trap, since it becomes possible to

Rapidly Rotating Bose-Einstein Condensates

rotate the system arbitrarily fast. As the system rotates sufficiently rapidly, the centrifugal force pushes the particles towards the edge of the trap, and a hole open up in the center. Singly quantized vortex arrays with a hole have been seen in numerical simulations³¹ and discussed theoretically in Refs. 11,32,33,34,35. In addition, at very high rotation, systems tend to form a single multiply quantized vortex at the center, with order parameter $\psi \sim e^{i\nu\phi}$, where the integer quantization index ν is $\gg 1$. Such giant vortices have been seen in numerical simulations^{31,36}, and are discussed theoretically in Refs. 11,32,33,34. The schematic phase diagram, as a function of interparticle interaction strength vs. rotation rate is shown in Fig. 3. Full details can be found in Refs. 32,33,34,35. Initial studies of rapidly rotating condensates in harmonic lattices at the ENS are reported in Ref. 37.

ACKNOWLEDGMENTS

The research reported here grew out of collaborations with Chris Pethick, Uwe Fischer, Drew Gifford and Gentaro Watanabe, and was supported in part by NSF Grants PHY00-98353 and PHY03-55014. I am very grateful to Eric Cornell, Ian Coddington, Peter Engels, and Volker Schweikhard of JILA for many illuminating discussions of their experiments on rapidly rotating Bose condensates.

REFERENCES

1. G.A. Williams and R.E. Packard, *Phys. Rev. Lett.* **33**, 280 (1974); **33**, 459 (1978); E.J. Yarmchuk, M.J.V. Gordon, and R.E. Packard, *Phys. Rev. Lett.* **43**, 214 (1979); E.J. Yarmchuk and R.E. Packard, *J. Low Temp. Phys.* **46**, 479 (1982).
2. M.R. Matthews, B.P. Anderson, P.C. Haljan, D.S. Hall, C.E. Wieman, and E.A. Cornell, *Phys. Rev. Lett.* **83**, 2498 (1999).
3. K.W. Madison, F. Chevy, W. Wohlleben, and J. Dalibard, *Phys. Rev. Lett.* **84**, 806 (2000); F. Chevy, K.W. Madison, and J. Dalibard, *Phys. Rev. Lett.* **85**, 2223 (2000); K.W. Madison, F. Chevy, V. Bretin, and J. Dalibard, *Phys. Rev. Lett.* **86**, 4443 (2001).
4. J.R. Abo-Shaeer, C. Raman, J.M. Vogels, and W. Ketterle, *Science* **292**, 476 (2001).
5. P.C. Haljan, I. Coddington, P. Engels, and E.A. Cornell, *Phys. Rev. Lett.* **87**, 210403 (2001); P. Engels, I. Coddington, P.C. Haljan, and E.A. Cornell, *Phys. Rev. Lett.* **89**, 100403 (2002).
6. I. Coddington, P. Engels, V. Schweikhard, and E. Cornell, *Phys. Rev. Lett.* **91**, 100402 (2003).
7. V. Schweikhard, I. Coddington, P. Engels, V.P. Mogendorff, and E.A. Cornell, *Phys. Rev. Lett.* **92**, 040404 (2004)

G. Baym

8. I. Coddington, P. C. Haljan, P. Engels, V. Schweikhard, S. Tung and E. A. Cornell, cond-mat/0405240.
9. A.L. Fetter, *Phys. Rev. A* **64**, 063608 (2001).
10. However, within a few nanokelvin of the lambda point, where the coherence length becomes macroscopic, the behavior of the vortices as they become closely packed becomes a practicable and very interesting experiment. I am grateful to Robert Duncan for pointing out this possibility.
11. U.R. Fischer and G. Baym, *Phys. Rev. Lett.* **90**, 140402 (2003).
12. G. Baym and C.J. Pethick, *Phys. Rev. A* **69**, 043619 (2004).
13. T.-L. Ho, *Phys. Rev. Lett.* **87**, 060403 (2001).
14. G. Watanabe, G. Baym, and C. J. Pethick, cond-mat/0403470.
15. G. Baym and C. J. Pethick, *Phys. Rev. Lett.* **76** 6 (1996).
16. Similar arguments on the relation of the vortex density and the inhomogeneity of the density profile in the LLL regime have been given by A. MacDonald (private communication) and N.R. Cooper, S. Komineas, N. Read, cond-mat/0404112; and for slow rotation by J. Anglin (private communication; also Ref. 17, and D.E. Sheehy and L. Radzihovsky, cond-mat/0402637.
17. J.R. Anglin and M. Crescimanno, cond-mat/0210063.
18. V.K. Tkachenko, *Zh. Eksp. Teor. Fiz.* **49**, 1875 (1965); **50**, 1573 (1966); **56**, 1763 (1969) [*Sov. Phys. JETP* **22**, 1282 (1966); **23**, 1049 (1966); **29**, 245 (1969)].
19. C.D. Anderock and W.I. Glaberson, *J. Low Temp. Phys.* **48**, 257 (1982).
20. G. Baym and E. Chandler, *J. Low Temp. Phys.* **50**, 57 (1983); **62**, 119 (1986).
21. G. Baym, *Phys. Rev.* **B51**, 11697 (1995).
22. G. Baym, *Phys. Rev. Lett.* **91** 110402 (2003).
23. G. Baym, *Phys. Rev. A* **69**, 043618 (2004).
24. See M. Cozzini, L. Pitaevskii, and S. Stringari, *Phys. Rev. Lett.* **92**, 220401 (2004), for a derivation of the Tkachenko modes in realistic geometry in terms of the compressibility and f-sum rules.
25. J. Sinova, C.B. Hanna, and A.H. MacDonald, *Phys. Rev. Lett.* **89**, 030403 (2002).
26. S.A. Gifford and G. Baym, cond-mat/0405182, *Phys. Rev. A* (in press) 2004.
27. N.K. Wilkin, J.M.F. Gunn, and R.A. Smith, *Phys. Rev. Lett.* **80**, 2265 (1998); N.K. Wilkin and J.M.F. Gunn, *Phys. Rev. Lett.* **84**, 6 (2000); N.R. Cooper, N.K. Wilkin, J.M.F. Gunn, *Phys. Rev. Lett.* **87**, 120405 (2001).
28. S. Viefers, T.H. Hansson, and S.M. Reimann, *Phys. Rev. A* **62**, 053604 (2000).
29. J.W. Reijnders, F.J.M. van Lankvelt, K. Schoutens, and N. Read, *Phys. Rev. Lett.* **89**, 120401 (2002); *Phys. Rev.* **A69**, 023612 (2004).
30. N. Regnault and Th. Jolicoeur, cond-mat/0406013.
31. K. Kasamatsu, M. Tsubota, and M. Ueda, *Phys. Rev. A* **66**, 053606 (2002).
32. G.M. Kavoulakis and G. Baym, *New J. Phys.* **5**, 51.1 (2003).
33. A.D. Jackson and G.M. Kavoulakis, *Phys. Rev. A* **70**, 023601 (2004).
34. A.D. Jackson, G.M. Kavoulakis, and E. Lundh, *Phys. Rev. A* **69**, 053619 (2004).
35. G.M. Kavoulakis, G. Baym, and A.D. Jackson, cond-mat/0405658, *Phys. Rev. A* (in press).
36. E. Lundh, *Phys. Rev. A* **65**, 043604 (2002).
37. V. Bretin, S. Stock, Y. Seurin and, J. Dalibard, *Phys. Rev. Lett.* **92**, 050403 (2004).